ISSN 1063-7761, Journal of Experimental and Theoretical Physics, 2016, Vol. 123, No. 6, pp. 1060–1067. © Pleiades Publishing, Inc., 2016.
Original Russian Text © V.G. Peschanskii, O. Galbova, R. Hasan, 2016, published in Zhurnal Eksperimental'noi i Teoreticheskoi Fiziki, 2016, Vol. 150, No. 6, pp. 1218–1226.

ELECTRONIC PROPERTIES OF SOLID

Magnetic-Breakdown Oscillations of the Thermoelectric Field in Layered Conductors

V. G. Peschanskii[a,b]*, O. Galbova[c], and R. Hasan[a,d]

[a] *Karazin Kharkov National University, Kharkov, 61022 Ukraine*

[b] *Verkin Institute for Low-Temperature Physics and Engineering, National Academy of Sciences of Ukraine, Kharkov, 61103 Ukraine*

[c] *St. Cyril and Methodium University, P. O. Box 162, Skopie, 1000 Republic of Macedonia*

[d] *Physics Department, Birzeit University, P. O. Box 14, Birzeit, West Bank, Palestine*

**e-mail: vpeschansky@ilt.kharkov.ua*

Received May 19, 2016

Abstract—The response of an electron system to nonuniform heating of layered conductors with an arbitrary quasi-two-dimensional electron energy spectrum in a strong magnetic field **B** is investigated theoretically in the case when cyclotron frequency ω_c is much higher than the frequency $1/\tau$ of collisions between charge carriers. In the case of a multisheet Fermi surface (FS), we calculate the dependence of the thermoelectric coefficients on the magnitude and orientation of the magnetic field in the vicinity of the Lifshitz topological transition when the FS connectivity changes under the action of an external force (e.g., pressure) on the conductor. Upon a decrease in the spacing between individual pockets (sheets) of the FS, conduction electrons can tunnel as a result of the magnetic breakdown from one FS sheet to another; their motion over magnetic-breakdown trajectories becomes complicated and entangled. The thermoelectric field exhibits a peculiar dependence on the magnetic field: for a noticeable deviation of vector **B** from the normal through angle ϑ to the layers, the thermoelectric field oscillates as a function of $\tan\vartheta$. The period of these oscillations contains important information on the distance between individual FS sheets and their corrugation.

DOI: 10.1134/S1063776116110273

The energy spectrum of elementary excitations in crystals contains a number of critical values of energy ε_k, at which the topological structure (connectivity) of constant-energy energy surfaces $\varepsilon(\mathbf{p}) = \text{const}$ changes. At low temperatures T, thermodynamic and kinetic characteristics of the conduction electron system in degenerate conductors mainly depend on the structure of the Fermi surface (FS), $\varepsilon(p) = \varepsilon_F$ to within small corrections proportional to $(T/\varepsilon_F)^2$. Although critical energy levels ε_k are separated considerably from the Fermi level as a rule, the electronic topological transition in degenerate conductors can still be clearly observed when the chemical potential μ of conduction gradually can be varied continuously by gradually bringing it to ε_k (for example, by applying a high pressure or by doping the conductor with impurity atoms). This topological transition predicted by Lifshitz [2] was soon observed and thoroughly investigated experimentally for many metals and alloys in the normal and superconducting states [3–21]. Detailed information on these experiments can be found in Supplement to I.M. Lifshitz works written by Zavaritskii [22]. During last three decades, the interest in experimental investigations of the electronic topological transition was switched to MIS, nanostructures, and other low-dimensional current-conducting systems. The interest in such research persists even now. It turned out that the Lifshitz topological electronic transitions can be detected most simply and reliably using thermoelectric phenomena. We consider the linear response of the electron system of a layered conductor to a perturbation by electric field **E** and temperature gradient $\partial T/\partial \mathbf{r}$ in the vicinity of the electronic topological transition in the case when upon the convergence of individual FS pockets (sheets), conduction electrons can roam over various FS pockets. Following [23], we assume that a quasi-2D electron energy spectrum of a layered conductor

$$\varepsilon(\mathbf{p}) = \sum_{n=0}^{\infty} \varepsilon_n(p_x, p_y) \cos\left(\frac{anp_z}{\hbar} + \alpha_n(p_x, p_y)\right), \quad (1)$$

$$\begin{aligned} \varepsilon_n(-p_x, -p_y) &= \varepsilon_n(p_x, p_y), \\ \alpha_n(-p_x, -p_y) &= -\alpha_n(p_x, p_y) \end{aligned} \quad (2)$$

is arbitrary and its FS consists of topologically different elements in the form of cylinders and planar sheets weakly corrugated along momentum projection $p_z =$

$\mathbf{n} \cdot \mathbf{p}$ onto normal $\mathbf{n}$ to the layers. For definiteness, we direct the p_x axis orthogonally to quasi-2D FS sheets.

Here, a is the distance between the layers, $\hbar$ is the Planck constant, and $\varepsilon_n(p_x, p_y)$ and $\alpha(p_x, p_y)$ are arbitrary functions of their arguments such that all functions $\varepsilon_n(p_x, p_y)$ with $n \neq 0$ are much smaller than $\varepsilon_0(p_x, p_y)$ because the electron velocity

$$v_z = -\sum_{n=1}^{\infty} \frac{an}{\hbar} \varepsilon_n(p_x, p_y) \times \sin\left\{\frac{anp_z}{\hbar} + \alpha_n(p_x, p_y)\right\} \leq \eta v_F \quad (3)$$

along the normal to the layers is much smaller than the characteristic Fermi velocity v_F for an electron moving along the layers. In low-dimensional complexes of organic origin, parameter η of quasi-two-dimensionality of the electron energy spectrum is on the order of 10^{-2}, which facilitates the clearest manifestation of oscillatory effects in low-dimensional conductors.

We can determine electric current density

$$j_i = \sigma_{ij} E_j - \alpha_{ij} \partial T / \partial x_j \quad (4)$$

and heat flux

$$q_i = \beta_{ij} E_j - \chi_{ij} \partial T / \partial x_j \quad (5)$$

by solving the kinetic equation for the charge carrier distribution function

$$f(\mathbf{p}, \mathbf{r}) = f_0(\varepsilon) - \left(\phi - \frac{\varepsilon - \mu}{T}\psi\right)\frac{\partial f_0(\varepsilon)}{\partial \varepsilon} \times \left\{e\mathbf{E} \cdot \mathbf{v} - \frac{\varepsilon - \mu}{T}\mathbf{v}\frac{\partial T}{\partial \mathbf{r}} - \left(\frac{\partial \phi}{\partial t} - \frac{\varepsilon - \mu}{T}\frac{\partial \psi}{\partial t}\right)\frac{\partial f_0(\varepsilon)}{\partial \varepsilon}\right\} = \hat{W}\{f(\mathbf{p}, \mathbf{r}) - f_0(\varepsilon)\}. \quad (6)$$

Here,

$$f_0(\varepsilon) = \left(1 + \exp\frac{\varepsilon - \mu}{T}\right)^{-1}$$

is the equilibrium Fermi distribution function for conduction electrons and T is the temperature in energy units. For variables in the momentum space, we are using the integrals of motion of a charge in magnetic field $\mathbf{B}$ and time t of its motion in trajectory $\varepsilon = \text{const}$ and $p_B = \mathbf{p} \cdot \mathbf{B}/B = \text{const}$. On the left-hand side of kinetic equation (6), we have omitted the terms quadratic in the weak perturbation of the electron system. In the same approximation, collision integral $\hat{W}$ is the sum of two linear operators acting on sought functions ϕ and ψ.

We must seek the solution to Eq. (6) in the space of the eigenfunctions of integral operator $\hat{W}$. The relaxation time in the system of charge carriers is equal to the reciprocal of the smallest eigenvalue of the collision operator, the relaxation times τ and τ_ε in the direction of momenta and in energies being essentially different. These times are approximately identical only at very low temperatures at which charge carriers are scattered mainly by impurity atoms and other crystal lattice defects. However, upon an increase in temperature, the additional mechanism of electron scattering from thermal vibrations of ions in the crystal becomes operative, leading to different temperature dependences of relaxation times τ_ε and τ in the temperature range below the Debye temperature T_D. If we disregard numerical factors on the order of unity, it is expedient to use the τ approximation for the collision integral. Then kinetic equation (6) can be written as the system of two first-order ordinary differential equations

$$\frac{\partial \phi}{\partial t} + \frac{\phi}{\tau} = e\mathbf{E} \cdot \mathbf{v}, \quad (7)$$

$$\frac{\partial \psi}{\partial t} + \frac{\psi}{\tau_\varepsilon} = \mathbf{v}\frac{\partial T}{\partial \mathbf{r}}. \quad (8)$$

Using these equations and

$$\phi(t) = \int_{\lambda_1}^{t} dt' e\mathbf{E} \cdot \mathbf{v}(t') \exp\frac{t' - t}{\tau} + \exp\frac{\lambda_1 - t}{\tau}\phi(\lambda_1 + 0), \quad (9)$$

$$\psi(t) = \int_{\lambda_1}^{t} dt' \mathbf{v}(t')\left(\frac{\partial T}{\partial \mathbf{r}}\right)\exp\frac{t' - t}{\tau_\varepsilon} + \exp\frac{\lambda_1 - t}{\tau_\varepsilon}\psi(\lambda_1 + 0) \quad (10)$$

we obtain the electric current density

$$j_i = -\int \frac{2eB}{(2\pi\hbar)^3 c}\frac{\partial f_0(\varepsilon)}{\partial \varepsilon}\int dp_B \times \int_0^{T_B} dt e v_i(t)\left[\phi(t) - \frac{\varepsilon - \mu}{T}\psi(t)\right] \quad (11)$$

and heat flux

$$q_i = -\int \frac{2eB}{(2\pi\hbar)^3 c} d\varepsilon \frac{\partial f_0(\varepsilon)}{\partial \varepsilon}\int dp_B \times \int_0^{T_B} dt(\varepsilon - \mu) v_i(t)\left[\phi(t) - \frac{\varepsilon - \mu}{T}\psi(t)\right]. \quad (12)$$

Here, e, $\mathbf{v}$, and T_B are the charge, velocity, and period of motion of conduction electrons in trajectory $\varepsilon(\mathbf{p}) = \text{const}$, $p_B = \text{const}$; c is the velocity of light, and $\hbar$ is the Planck constant.

Functions $\phi(\lambda_1 + 0)$ and $\psi(\lambda_1 + 0)$ describe a complex motion of charge carriers in magnetic-breakdown trajectories with magnetic breakdown probability w in region A and probability w' in region B of convergence of individual FS pockets at instants λ_1, λ_2, λ_3, λ_4, where λ_1 is the closest to t instant of an electron transition from one FS sheet to another with the conservation of integral of motion p_B, and $\lambda_k > \lambda_{k+1}$ (see

Fig. 1). For example, the nonequilibrium part of the electron distribution function in FS sheet *1* after a magnetic breakdown in the vicinity of point *A*,

$$\phi_1(\lambda_1 + 0) = \int\limits_{-\infty}^{\lambda_i} dt \exp\frac{t-\lambda_1}{\tau}(e\mathbf{E}\cdot\mathbf{v}(t))_1 \qquad (13)$$

is connected with the electron distribution function $\phi_1(\lambda_1 + 0)$ in the same channel prior to the magnetic breakdown by the following relation:

$$\phi_1(\lambda_1 + 0) = (1-w)\phi_1(\lambda_1 - 0) + w\phi_2(\lambda_1 - 0). \qquad (14)$$

Function $\phi_i(\lambda_j - 0)$ before the magnetic breakdown at instant λ_j is connected with function $\phi_i(\lambda_{j+1} + 0)$ after the magnetic breakdown at an earlier instant λ_{j+1} by the following simple relation:

$$\phi_i(\lambda_j - 0) = A_i + \exp\left(\frac{\lambda_{j+1} - \lambda_j}{\tau}\right)\phi_i(\lambda_{j+1} + 0), \qquad (15)$$

where

$$A_i = \int\limits_{\lambda_{j+1}}^{\lambda_{j1}} dt \exp\frac{t-\lambda_j}{\tau}(e\mathbf{E}\cdot\mathbf{v}(t))_i, \qquad i = 1,2,3,4 \qquad (16)$$

is the energy acquired by a conduction electron in the electric field during its motion over the *i*th FS sheet over time $(\lambda_j - \lambda_{j+1})$ between two magnetic breakdown events, which is equal to T_1 for electrons on planar FS sheets *1* and *3* and to T on arcs *2* and *4* of the closed cross section of the corrugated cylinder. To within small corrections proportional to parameter η, time T_1 of the quasi-periodic motion of charge carriers in the magnetic field on FS sheets *1* and *3* is independent of λ_j. In the same approximation in the small quasi-two-dimensionality parameter η of the electron energy spectrum, functions A_i are identical for any value of λ_j.

Taking into account relations (14) and (15), we can write the relation connecting function $\phi_1(\lambda_1 + 0)$ with functions ϕ_1 and ϕ_2 at an earlier instant λ_2 in the form

$$\phi_1(\lambda_1 + 0) = Q_1 + h_1\phi_1(\lambda_2 + 0) + g\phi_2(\lambda_2 + 0). \qquad (17)$$

Analogously, at earlier instants λ_2, λ_3, λ_4, and λ_5, we obtain

$$\phi_2(\lambda_2 + 0) = Q_4 + h'\phi_4(\lambda_3 + 0) + g_1'\phi_3(\lambda_3 + 0), \qquad (18)$$

$$\phi_3(\lambda_3 + 0) = Q_3 + h_1'\phi_3(\lambda_4 + 0) + g'\phi_4(\lambda_4 + 0), \qquad (19)$$

$$\phi_4(\lambda_4 + 0) = Q_2 + h\phi_2(\lambda_5 + 0) + g_1'\phi_1(\lambda_5 + 0), \qquad (20)$$

$$\phi_1(\lambda_5 + 0) = Q_1 + h_1\phi_1(\lambda_6 + 0) + g\phi_2(\lambda_6 + 0). \qquad (21)$$

Here,

$$Q_1 = (1-w)A_1 + wA_2, \quad Q_2 = (1-w)A_2 + wA_1, \quad Q_3 = (1-w')A_3 + w'A_4, \quad Q_4 = (1-w')A_4 + w'A_3, \qquad (22)$$

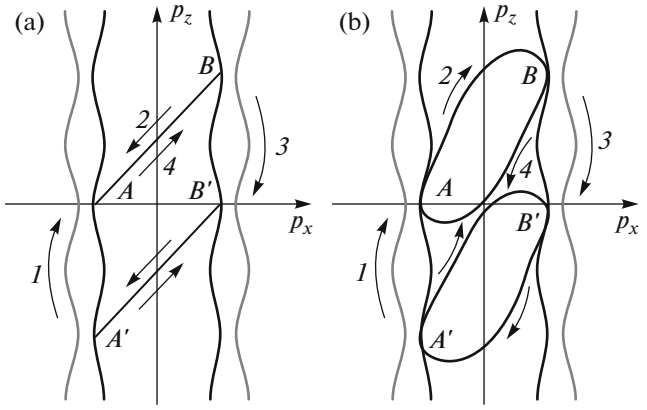

Fig. 1. Projection of electron trajectories onto the p_xp_z plane (a) and in a magnetic field tilted from this plane (b).

$$h_1 = (1-w)\exp\left(-\frac{T_1}{\tau}\right), \quad h_1' = (1-w')\exp\left(-\frac{T_1}{\tau}\right), \quad g_1 = w\exp\left(-\frac{T_1}{\tau}\right), \quad g_1' = w'\exp\left(-\frac{T_1}{\tau}\right), \quad h = (1-w)\exp\left(-\frac{T'}{\tau}\right), \quad h' = (1-w')\exp\left(-\frac{T'}{\tau}\right), \quad g = w\exp\left(-\frac{T'}{\tau}\right), \quad g' = w'\exp\left(-\frac{T'}{\tau}\right). \qquad (23)$$

It can easily be seen that relation (21) differs from (17) only in the earlier instant of magnetic breakdown. Continuing the recurrent relations, we proceed to the remote past because the sought functions on the right-hand sides of the equations for each recurrence acquire factors smaller than unity and become infinitely small after multiple recurrence. As a result, functions ϕ_i on the left-hand side of Eqs. (17)–(20) can be represented by an infinite series of terms proportional to A_j, which form a geometrical progression that can easily be summed.

Using recurrent relations for Eqs. (17) and (19), we obtain

$$\phi_1(\lambda_1 + 0) = \frac{Q_1}{1-h_1} + \sum_{n=0}^{\infty} h_1^n g\phi_2(\lambda_{n+2} + 0), \qquad (24)$$

$$\phi_3(\lambda_j + 0) = \frac{Q_3}{1-h_1'} + \sum_{n=0}^{\infty} (h_1')^n g'\phi_4(\lambda_{n+j+1} + 0). \qquad (25)$$

Using relation (20) for function ϕ_4, we can find the relation between function $\phi_3(\lambda_j + 0)$ and functions ϕ_2 at different instants λ_n:

$$\phi_3(\lambda_j + 0) = \frac{Q_3}{1-h_1'} + \frac{g_1 g' Q_1}{(1-h_1)(1-h_1')} + \frac{g' Q_2}{1-h_1'} + \sum_{n=0}^{\infty} (h_1')^n g' h \phi_2(\lambda_{n+j+2} + 0) + \sum_{n,k=0}^{\infty} (h_1')^n h_1^k g_1 g g' h \phi_2(\lambda_{n+k+j+4} + 0). \quad (26)$$

Using relations (24)–(26), we obtain the following functional equation for function $\phi_2(\lambda_2 + 0)$:

$$\phi_2(\lambda_2 + 0) = hh' \phi_2(\lambda_4 + 0) + Q_4 + h' Q_2 + g_1' \left[\frac{Q_3}{1-h_1'} + \frac{g_1 g' Q_1}{(1-h_1)(1-h_1')} + \frac{g' Q_2}{1-h_1'} \right] + h' g_1 \frac{Q_1}{1-h_1} + \sum_{n=0}^{\infty} (h_1')^n g' g_1' h \phi_2(\lambda_{n+j+2} + 0) + h' g_1 \sum_{n=0}^{\infty} h_1^n g \phi_2(\lambda_{n+2} + 0) + \sum_{n,k=0}^{\infty} (h_1')^n h_1^k g_1 g g' g_1' h \phi_2(\lambda_{n+k+j+4} + 0). \quad (27)$$

Applying the recurrent transformation to Eq. (27), we acquire additional summation over powers of parameter hh'. As a result, the functional equation for function $\phi_2(\lambda_j + 0)$ assumes the final form for any initial magnetic breakdown instant λ_j,

$$\phi_2(\lambda_j + 0) = \frac{[Q_1 g_1 + Q_2(1-h_1)](h'(1-h_1') + g' g_1')}{(1-hh')(1-h_1)(1-h_1')} + \frac{[Q_3 g_1' + Q_4(1-h_1')](1-h_1)}{(1-hh')(1-h_1)(1-h_1')} + \hat{L}\phi_2(\lambda_j), \quad (28)$$

where

$$\hat{L}\phi_2(\lambda_1 + 0) = \sum_{n,k,m=0}^{\infty} (hh')^m (h_1')^n h_1^k g_1 g g' g_1' h \phi_2(\lambda_{n+k+m+10} + 0) + \sum_{n,m=0}^{\infty} (hh')^m (h_1')^m g' g_1' h \phi_2(\lambda_{n+m+7} + 0) + \sum_{n,m=0}^{\infty} (hh')^m h_1^n h' g_1 g \phi_2(\lambda_{n+m+7} + 0). \quad (29)$$

The solution to this equation is a geometrical progression with ratio q equal to the eigenvalue of linear operator $\hat{L}\phi_0 = q\phi_0$,

$$q = \frac{g g' g_1 g_1' + g_1' g' h(1-h_1) + g g_1 h'(1-h_1')}{(1-hh')(1-h_1)(1-h_1')}. \quad (30)$$

Summing the progression with allowance for relations (22) and (23), we obtain the following relation for $\phi_2(\lambda_j + 0)$:

$$\phi_2(\lambda_j + 0) = \frac{[A_1 w(1+\gamma_1) + A_2(w(1-\gamma_1)+\gamma_1)](w'(1-\gamma_1)+\gamma_1)}{2ww'(\gamma+\gamma_1) + (w+w')\gamma_1(\gamma_1+2\gamma) + 2\gamma\gamma_1^2} + \frac{[A_3 w'(1+\gamma_1) + A_4(w'(1-\gamma_1)+\gamma_1)](w+\gamma_1)(1+\gamma)}{2ww'(\gamma+\gamma_1) + (w+w')\gamma_1(\gamma_1+2\gamma) + 2\gamma\gamma_1^2}, \quad (31)$$

where $\gamma = \exp(T'/\tau) - 1$ and $\gamma_1 = \exp(T_1/\tau) - 1$.

Using relations (20)–(24), we obtain

$$\phi_1(\lambda_j + 0) = \frac{1+\gamma_1}{w+\gamma_1}\{(1-w)A_1 + wA_2\} + \frac{w}{w+\gamma_1}\phi_2(\lambda_j + 0), \quad (32)$$

$$\phi_3(\lambda_j + 0) = \frac{1+\gamma_1}{w'+\gamma_1}\{(1-w')A_3 + w'A_4\} + \frac{w'}{w'+\gamma_1}\phi_4(\lambda_j + 0), \quad (33)$$

$$\phi_4(\lambda_j + 0) = \phi_2(\lambda_j + 0) + A_1 + A_2 - \frac{\gamma_1 w}{w+\gamma_1}\phi_2(\lambda_j + 0) - \frac{\gamma_1}{w+\gamma_1}\{(1-w)A_1 + wA_2\}. \quad (34)$$

It can easily be seen that function $\phi_2(\lambda_j + 0)$ for small γ and γ_1 in inversely proportional to $(\gamma + \gamma_1)$, and all terms in formula (34) except the first are small corrections to it for $(\gamma + \gamma_1) \ll 1$.

Using relations (9)–(12) and (31)–(34) for an arbitrary orientation of magnetic field $\mathbf{B} = (B\cos\varphi\sin\vartheta, B\sin\varphi\sin\vartheta, B\cos\vartheta)$, we can determine all kinetic coefficients of the conductor; in particular, the electrical conductivity tensor has the form

$$\sigma_{ij}(\mu) = \frac{2e^3 B}{c(2\pi\hbar)^3} \int dp_B \sum_{k=1}^{4} \int_0^{T_k} dt v_{ik}(t) \times \left\{ \int_{\lambda_1}^{t} dt' \exp\frac{t'-t}{\tau} v_{jk}(t', p_B) + \exp\frac{\lambda_1 - t}{\tau} u_{jk}(\lambda_1, p_B) \right\}, \quad (35)$$

where $e\mathbf{E}\cdot\mathbf{u}_{\mathbf{k}}(\lambda_1, p_B) = \phi_k(\lambda_1 + 0, p_B)$, and k is the index of summation over all regions of the magnetic-breakdown trajectory of charge carriers, $k = 1, 2, 3, 4$; $T_3 = T_1$ and $T_2 = T_4 = T$.

To within small corrections proportional to $(T/\mu)^2$, we obtain the following expressions for the thermoelectric coefficients:

$$\beta_{ij} = \frac{\pi^2}{3e} T^2 \frac{d\sigma_{ij}(\mu)}{d\mu}, \quad (36)$$

$$\alpha_{ij} = \frac{\pi^2}{3e} T \frac{d\sigma'_{ij}(\mu)}{d\mu}, \quad (37)$$

where tensor $\sigma'_{ij}(\mu)$ coincides with tensor $\sigma_{ij}(\mu)$ if electron relaxation time τ in the directions of the momentum in it is replaced by the electron energy relaxation time τ_ε.

Analogously, we can write the thermal conductivity tensor components:

$$\chi_{ij} = -\int \sigma'_{ij}(\varepsilon) \frac{(\varepsilon - \mu)^2}{e^2 T} \frac{\partial f_0(\varepsilon)}{\partial \varepsilon} d\varepsilon = \frac{\pi^2}{3e^2} T \sigma'_{ij}(\mu). \quad (38)$$

It is undoubtedly interesting to consider the case of a long mean free path of conduction electrons or a strong magnetic field, when the values of quantities γ and γ_1 (which are approximately of the same order of magnitude) are so small that it is sufficient to confine analysis to the asymptotic approximation for kinetic coefficients $w \gg \gamma$ and $w' \gg \gamma_1$. In this approximations, functions $\phi_i(\lambda_j + 0)$ assume the form

$$\phi_2(\lambda_j + 0) = \phi_4(\lambda_j + 0) = \frac{A_1 + A_2 + A_3 + A_4}{2(\gamma + \gamma_1)}, \quad (39)$$

$$\phi_1(\lambda_1 + 0) = \frac{(1 - w)A_1}{w} + \frac{A_1 + A_2 + A_3 + A_4}{2(\gamma + \gamma_1)}, \quad (40)$$

$$\phi_3(\lambda_1 + 0) = \frac{(1 - w')A_3}{w'} + \frac{A_1 + A_2 + A_3 + A_4}{2(\gamma + \gamma_1)}. \quad (41)$$

The first terms on the right-hand sides of asymptotic formulas (40) and (41) are much smaller than the last terms, and a conduction electron "visits" all channels of the magnetic-breakdown trajectory with the same probability; in other words, in each occasion of a magnetic breakdown, the electron as if necessarily passes to another FS sheet (see Fig. 2) and performs periodic motion with period $2(T_1 + T)$.

The asymptotic expressions for $\sigma_{ij}(\varepsilon)$ and $\sigma'_{ij}(\varepsilon)$ have the form

$$\sigma_{ij}(\varepsilon) = \frac{2e^3 B}{c(2\pi\hbar)^3} \int \frac{\tau dp_B}{2(T' + T_1)} \times \{T_1(\overline{v_{i1} + v_{i3}}) + T'(\overline{v_{i2} + v_{i4}})\} \times \{T_1(\overline{v_{j1} + v_{j3}}) + T'(\overline{v_{j2} + v_{j4}})\}, \quad (42)$$

$$\sigma'_{ij}(\varepsilon) = \frac{2e^3 B}{c(2\pi\hbar)^3} \int \frac{\tau_\varepsilon dp_B}{2(T' + T_1)} \times \{T_1(\overline{v_{i1} + v_{i3}}) + T'(\overline{v_{i2} + v_{i4}})\} \times \{T_1(\overline{v_{j1} + v_{j3}}) + T'(\overline{v_{j2} + v_{j4}})\} \quad (43)$$

and can be readily used for calculating the thermoelectric field generated by the temperature gradient in the absence of current leads:

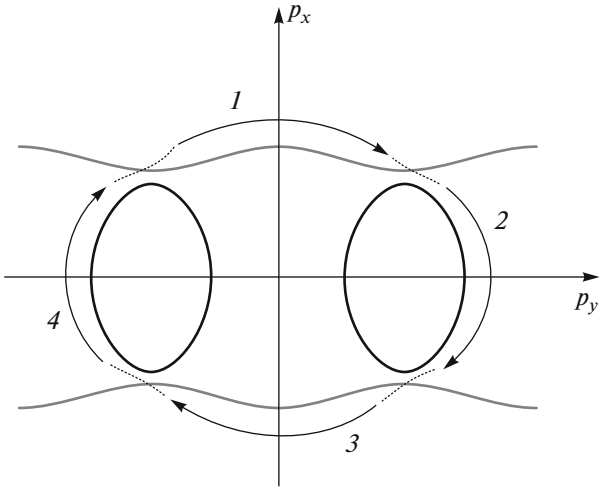

Fig. 2. Projection of electron trajectories onto the $p_x p_y$ plane in a magnetic field.

$$E_i = \frac{\pi^2 T}{3e} \rho_{ik} \frac{\partial \sigma'_{kj}(\mu)}{\partial \mu} \frac{\partial T}{\partial x_j}. \quad (44)$$

The main contribution to the thermoelectric field along the normal to the layers,

$$E_z = \frac{\pi^2 T}{3e} \rho_{zz} \frac{d\sigma'_{zj}(\mu)}{d\mu} \frac{\partial T}{\partial x_j} + \frac{\pi^2 T}{3e} \left\{ \rho_{zx} \frac{d\sigma'_{xj}(\mu)}{d\mu} + \rho_{zy} \frac{d\sigma'_{yj}(\mu)}{d\mu} \right\} \frac{\partial T}{\partial x_j} \quad (45)$$

comes from the first term because the resistivity tensor component ρ_{zz} equal to $1/\sigma_{zz}$ considerably exceeds all the remaining components of tensor ρ_{ij} in the main approximation in parameter η.

The electrical conductivity tensor components σ'_{zx} and σ'_{zy} can easily be calculated using the equation of motion for charge carriers:

$$\frac{\partial p_x}{\partial t} = \frac{eB}{c}(v_y \cos j - v_z \sin\varphi \sin\vartheta), \quad (46)$$

$$\frac{\partial p_y}{\partial t} = \frac{eB}{c}(v_z \cos\varphi \cos\vartheta - v_x \cos\vartheta), \quad (47)$$

which gives

$$v_x = v_y \cos\varphi \tan\vartheta - \frac{c}{eB\cos\vartheta} \frac{\partial p_y}{\partial t}, \quad (48)$$

$$v_y = v_z \sin\varphi \tan\vartheta + \frac{c}{eB\cos\vartheta} \frac{\partial p_x}{\partial t}. \quad (49)$$

Since the charge carrier drifts on FS sheets *1* and *3* (as well as on FS sheets *2* and *4*) have opposite directions, the substitution of expressions (48) and (49) into expression (43) for σ'_{ij} gives the following asymptotic

expression for the thermoelectric field in a strong magnetic field when $\max\{\gamma, \gamma_1) \ll \min\{w, w'\}$:

$$E_z = \frac{\pi^2 T}{3e}\frac{\tau}{\tau_\eta}\frac{\partial\sigma_{zz}(\mu)}{\sigma_{zz}\partial\mu} \times\left(\frac{\partial T}{\partial z} + \cos\varphi\tan\vartheta\frac{\partial T}{\partial x} + \sin\varphi\tan\vartheta\frac{\partial T}{\partial y}\right). \quad (50)$$

For $\tan\vartheta \gg 1$, electron velocity v_z along the normal to the layers often changes its sign, and the main contribution to the period-averaged value of $\bar{v}_z$ comes from small neighborhoods in the vicinity of electron turning points, where

$$\frac{dp_z}{dt} = \frac{eB}{c}\sin\theta(v_x\sin\varphi - v_y\cos\varphi) = 0. \quad (51)$$

Simple calculations using the stationary phase method lead to the following asymptotic expression (for $\tan\vartheta \gg 1$) for the drift velocity of conduction electrons between two magnetic breakdown events:

$$\breve{v}_{zk} = -\sum_{n=1}^{\infty}\varepsilon_{nk}(t_1, p_B)\left|\frac{2\pi an}{p''_{zk}(t_1)\hbar}\right|^{1/2} T_k^{-1}\sin\left[\frac{an}{\hbar}p_{zk}^{\min} + \frac{\pi}{4}\right] -\sum_{n=1}^{\infty}\varepsilon_{nk}(t_2, p_B)\left|\frac{2\pi an}{p''_{zk}(t_2)\hbar}\right|^{1/2} T_k^{-1}\sin\left[\frac{an}{\hbar}p_{zk}^{\max} - \frac{\pi}{4}\right], \quad (52)$$

where $p''_{zk}(t)$ is the second derivative with respect to t at the stationary phase points, where $p_{zk}(t)$ is equal to its minimal value $p_{zk}^{\min}$ at $t = t_1$ and to it maximal value $p_{zk}^{\max}$ at $t = t_2$ on the kth FS sheet; $k = 1, 2, 3, 4$, and

$$p''_{zk}(t_1) = -[p''_{xk}(t_1)\cos\varphi + p''_{yk}(t_1)\sin\varphi]\tan\vartheta, \quad p''_{zk}(t_2) = -[p''_{xk}(t_2)\cos\varphi + p''_{yk}(t_2)\sin\varphi]\tan\vartheta. \quad (53)$$

All remaining charge carriers on the electron trajectory introduce only small corrections proportional to $(\tan\vartheta)^{-1/2}$ to $\breve{v}_{zk}$.

The distance $(p_{zk}^{\max} - p_{zk}^{\min})$ between the stationary phase points is proportional to $\tan\vartheta$, and the drift velocity of charge carriers in a strongly extended trajectory in the momentum space varies periodically as a function of $\tan\vartheta$; therefore, the period of these oscillations contains important information on the electron energy spectrum of charge carriers. With increasing angle ϑ, the electron drift velocity along the normal to the layers decreases, leading to a decrease in the electrical conductivity σ_{zz} between the layers in inverse proportion to $\tan\vartheta$; the differentiation of the rapidly oscillating component σ_{zz} with respect to μ leads to its multiplication by $\tan\vartheta$.

As a result, the amplitude of angular oscillations of even longitudinal thermoelectric field considerably exceeds the amplitude of oscillations of the resistivity in a magnetic field lying in the xz plane, which was calculated in [23]. In this case, the Nernst–Ettingshausen field experiences giant oscillations upon a change in $\tan\vartheta$, rapidly changing its direction.

The total drift velocity of charge carriers $(\breve{v}_{z1} + \breve{v}_{z3})$ on quasi-planar FS sheets and $(\breve{v}_{z2} + \breve{v}_{z4})$ in the cylindrical FS pocket has the form

$$\breve{v}_{z1} + \breve{v}_{z3} = 2\sum_{n=1}^{\infty}\sin\frac{an(p_{z1}^{\min} + p_{z3}^{\max})}{2\hbar} \times\left[a_{n1}\cos\left(\frac{an}{2\hbar}(p_{z1}^{\min} - p_{z3}^{\max}) + \frac{\pi}{4}\right) + a_{n2}\cos\left(\frac{an}{\hbar}(p_{z1}^{\max} - p_{z3}^{\min}) - \frac{\pi}{4}\right)\right], \quad (54)$$

$$\breve{v}_{z2} + \breve{v}_{z4} = \sum_{n=1}^{\infty}\left[b_{n1}\sin\left(\frac{an}{\hbar}p_{xc}^{\min} + \frac{\pi}{4}\right) + b_{n2}\sin\left(\frac{an}{\hbar}p_{xc}^{\max} - \frac{\pi}{4}\right)\right], \quad (55)$$

where $p_{zc}^{\max}$ and $p_{zc}^{\min}$ are the extremal values of the momentum projection on a closed cross section of the cylindrical part of the FS, and

$$a_{n1} = -\frac{an}{\hbar T_1}\{\varepsilon_n(p_{x1}(t_1, p_B), p_{y1}(t_1, p_B))\left|\frac{2\pi\hbar}{ap''_{z1}(t_1)}\right|^{1/2}, \quad (56)$$

$$a_{n2} = -\frac{an}{\hbar T_1}\{\varepsilon_n(p_{x1}(t_2, p_B), p_{y1}(t_2, p_B))\left|\frac{2\pi\hbar}{ap''_{z1}(t_2)}\right|^{1/2}, \quad (57)$$

$$b_{n1} = -\frac{an}{\hbar T'}\{\varepsilon_n(p_{x2}(t_1, p_B), p_{y2}(t_1, p_B))\left|\frac{2\pi\hbar}{ap''_{z2}(t_1)}\right|^{1/2}, \quad (58)$$

$$b_{n2} = -\frac{an}{\hbar T'}\{\varepsilon_n(p_{x2}(t_2, p_B), p_{y2}(t_2, p_B))\left|\frac{2\pi\hbar}{ap''_{z2}(t_2)}\right|^{1/2}. \quad (59)$$

Using expressions (54) and (55), we can easily calculate tensor component $\sigma'_{zz}(\mu)$:

$$\sigma'_{zz}(\mu) = \frac{\pi e^2\tau_\varepsilon}{a(2\pi\hbar)^2(m_1 + m_2)} \times\left\{\sum_{n=1}^{\infty}m_2^2\left[b_{n1}^2 + b_{n2}^2 + 2b_{n1}b_{n2}\sin\frac{a(p_{zc}^{\max} - p_{zc}^{\min})}{\hbar}\right] + \sum_{n=1}^{\infty}2m_1^2\left[a_{n1}^2\sin\frac{a(p_{z3}^{\max} - p_{z1}^{\min})}{\hbar} - a_{n2}^2\sin\frac{a(p_{z3}^{\min} - p_{z1}^{\max})}{\hbar} + 2a_{n1}a_{n2}\cos\frac{a(p_{z3}^{\max} - p_{z1}^{\min})}{\hbar}\right] + \sum_{n=1}^{\infty}2m_1^2\left[a_{n1}^2 + a_{n2}^2 + 2a_{n1}a_{n2}\sin\frac{a(p_{z1}^{\max} - p_{z1}^{\min})}{\hbar}\right]\right\} \quad (60)$$

$$+\sum_{n=1}^{\infty} m_1 m_2 (b_{n1} + b_{n2}) \left[a_{n1} \left(\cos \frac{an}{\hbar} (p_{z3}^{\max} - p_{zc}^{\min}) \right.\right.$$
$$\left. - \sin \frac{an}{\hbar} (p_{z1}^{\min} - p_{zc}^{\max}) \right) + a_{n2} \left(\cos \frac{an}{\hbar} (p_{z3}^{\min} - p_{zc}^{\min}) \right.$$
$$\left.\left. + \sin \frac{an}{\hbar} (p_{z1}^{\max} - p_{zc}^{\min}) \right) \right].$$

Here, m_1 and m_2 are the effective cyclotron masses of charge carriers on quasi-planar and cylindrical FS sheets.

It should be borne in mind that the above expressions are valid for a slight deviation of the magnetic field from the xz plane through angle φ, when there still exist stationary phase points on the trajectory of electrons moving in quasi-planar regions of the FS. With increasing φ, the stationary-phase points on each quasi-planar FS sheet gradually approach one another (see Fig. 3), and for $\varphi_0 = \arctan(v_y(t)/v_x(t))^{\max} \le \arctan(v_F/v_x^{\min})_0$, these points merge at $t = t_0$, where $p_z''(t_0) = p_z'(t_0) = 0$. In this case, magnetic-breakdown oscillations involving charge carriers moving over planar FS sheets are absent, and conventional angular oscillations of electrical conductivity across the layers at $\tan\vartheta \gg 1$ are contained only in the first term of expression (60). The period of conventional angular oscillations involving only electrons on the cylindrical part of the FS contains information on the extremal diameter of the cylinder along the axis deflected through angle φ from the p_x axis, and the amplitude of these oscillations has approximately the same form as in the absence of magnetic breakdown, but reduced by a factor of $2(m_1 + m_2)/m_2$.

However, the magnetic-breakdown oscillations of kinetic coefficients are most informative for $\varphi = 0$. For example, the contribution to the magnetic-breakdown oscillation from the kinetic coefficients for conduction electrons tunneling between cylindrical and planar FS sheets (the last term in formula (60)),

$$\delta\sigma_{zz}'(\mu) = \frac{\pi e^2 \tau_\varepsilon}{a(2\pi\hbar)^2 (m_1 + m_2)} \sum_{n=1}^{\infty} m_1 m_2 (b_{n1} + b_{n2})$$
$$\times [a_{n1} (\cos\alpha_n (\Delta_p + \delta p_x) + \sin\alpha_n (\Delta_p + \delta p_x + D_p)) \quad (61)$$
$$+ a_{n2} (\cos\alpha_n (\Delta_p + D_p) - \sin\alpha_n \Delta_p)],$$

contains important information on corrugation of δp_x of quasi-planar FS sheets and minimal distance Δ_p between these sheets and the weakly corrugated cylinder. Here, $\alpha_n = (an/\hbar)\tan\vartheta$ and D_p is the diameter of the cylinder along the p_x axis. In the differentiation of $\sigma_{zz}'(\mu)$ with respect to μ, there is no need to retain the derivatives of functions smoothly depending on μ with respect to μ; it is sufficient to confine analysis to the differentiation of only trigonometric functions in formulas (60) and (61), the arguments of which are proportional to $\tan\vartheta \gg 1$. As a result, oscillations of thermoelectric coefficient α_{zz} are giant by nature for $\tan\vartheta \gg 1$:

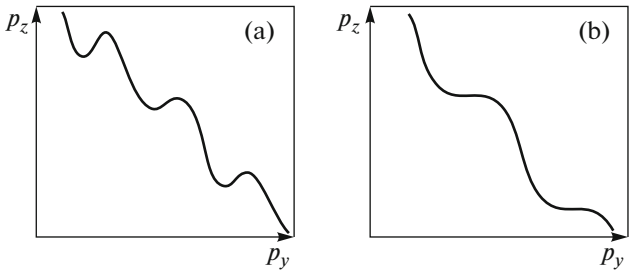

Fig. 3. Projection of electron trajectories onto the $p_y p_z$ plane in a magnetic field for (a) $\varphi < \varphi_0$ and (b) $\varphi = \varphi_0$.

$$\delta\alpha_{zz} = \frac{\pi^2}{3e} T \frac{d\delta\sigma_{zz}'(\mu)}{d\mu} = \frac{\pi^2 e \tau_\varepsilon T}{a(2\pi\hbar)^2 (m_1 + m_2)\varepsilon_F}$$
$$\times \sum_{n=1}^{\infty} m_1 m_2 (b_{n1} + b_{n2}) \tan\vartheta \quad (62)$$
$$\times [\beta_{n1} \cos\alpha_n (\Delta_p + \delta p_x + D_p) - \beta_{n3} \cos\alpha_n \Delta_p$$
$$- \beta_{n2} \sin\alpha_n (\Delta_p + D_p) - \beta_{n4} \sin\alpha_n (\Delta_p + \delta p_x)],$$

where β_{n1} and β_{n4} are equal to $n\alpha_{n1}$ to within a numerical factor on the order of unity, while β_{n1} and β_{n4} are equal to $n\alpha_{n2}$.

The detection of magnetic-breakdown angular oscillations of the thermoelectric field is a direct confirmation of the occurrence of the Lifshitz electronic topological transition. The interest in this problem continues unabated even today (see, for example, [24–32]).

Thermoelectric phenomena in low-dimensional conductors under pressure are being actively studied in many laboratories. Special attention is paid to organic charge-transfer complexes based on tetrathiafulvalene.

We strove to make this research helpful and available of experimenters. For this reason, we considered a multisheet FS typical of a large family of organic conductors including tetrathiafulvalene salts (BEDT-TTF)$_2$MHg(SCN)$_4$, where M = K, Rb, Tl; there are indications that quasi-planar sheets are weakly corrugated along the p_y axis also, and the energy spectrum of charge carriers in these FS sheets is quasi-one-dimensional [33].

We have confined our analysis to the semiclassical description of kinetic effects in the conditions of so-called incoherent magnetic breakdown according to the Slutskin classification [34, 35], in which temperature blurring $2\pi^2 T$ of quantized energy levels for electrons in a magnetic field is much larger than the spacing $\hbar\omega_c$ between these levels, and the complex form of quantum oscillations of kinetic coefficients does not prevent the observation of classical angular oscilla-

tions of magnetoresistance and thermoelectric effects. In this case, we can disregard the wave properties of an electron located during the magnetic breakdown in both regions of the magnetic-breakdown trajectory and confine our analysis to statistical probabilistic description of the dynamics of electron motion in magnetic-breakdown trajectories.

REFERENCES

1. L. van Hove, Phys. Rev. **89**, 1189 (1953).
2. I. M. Lifshits, Sov. Phys. JETP **11**, 1130 (1960).
3. M. A. Krivoglaz and Tyu Khao, Fiz. Met. Metalloved. **21**, 817 (1966).
4. V. G. Vaks, A. V. Trefilov, and S. V. Fomichev, Sov. Phys. JETP **53**, 830 (1981).
5. A. A. Varlamov and A. V. Pantsulaya, Sov. Phys. JETP **62**, 1263 (1985).
6. A. A. Abrikosov and A. V. Pantsulaya, Sov. Phys. Solid State **28**, 1195 (1986).
7. G. P. Mikitik and Yu. V. Sharlai, Phys. Rev. B **90**, 155122 (2014).
8. N. B. Brandt, N. I. Ginzburg, and T. A. Ignat'eva, Sov. Phys. JETP **22**, 61 (1965).
9. E. S. Itskevich and A. N. Voronovskii, JETP Lett. **4**, 151 (1966).
10. W. Chu et al., Phys. Rev. **131**, 214 (1970).
11. T. F. Smith, J. Low Temp. Phys. **11**, 584 (1973).
12. Yu. P. Gaidukov, N. P. Danilova, and M. B. Shcherbina-Samoilova, JETP Lett. **25**, 479 (1977).
13. Yu. P. Gaidukov, N. P. Danilova, and M. B. Shcherbina-Samoilova, Sov. J. Low Temp. Phys. **4**, 124 (1978).
14. Yu. P. Gaidukov, N. P. Danilova, and M. B. Shcherbina-Samoilova, Sov. Phys. JETP **50**, 1018 (1979).
15. D. R. Overcash et al., Phys. Rev. Lett. **46**, 287 (1981).
16. V. S. Egorov and A. N. Fedorov, Sov. Phys. JETP **58**, 959 (1983).
17. V. S. Egorov and S. R. Varyukhin, JETP Lett. **39**, 621 (1984).
18. S. L. Bud'ko, A. N. Voronovskii, A. G. Gaponchenko, and E. S. Itskevich, Sov. Phys. JETP **59**, 454 (1984).
19. N. V. Zavaritskii, V. I. Makarov, and A. A. Yurgens, JETP Lett. **42**, 182 (1985).
20. A. N. Velikodnyi, N. V. Zavaritskii, T. A. Ignat'eva, and A. A. Yurgens, JETP Lett. **43**, 773 (1986).
21. S. L. Bud'ko, A. G. Gaponchenko, and E. S. Itskevich, JETP Lett. **47**, 128 (1988).
22. N. V. Zavaritskii, in Selected Works of I. M. Lifshitz, Electronic Theory of Metals. Polymers and Biopolymers (Nauka, Moscow, 1994), Supplement, p. 432 [in Russian].
23. O. Galbova, V. G. Peschanskii, and D. I. Stepanenko, Low Temp. Phys. **41**, 537 (2015).
24. P. A. Goddard, S. J. Blundell, J. Singleton, et al., Phys. Rev. B **69**, 174509 (2004).
25. M. V. Kartsovnik, G. Andres, S. V. Simonov, W. Biberacher, I. Sheikin, N. D. Kushch, and H. Muller, Phys. Rev. Lett. **96**, 16601 (2006).
26. A. F. Bangura, P. A. Goddard, J. Singleton, et al., Phys. Rev. B **76**, 052510 (2007).
27. T. Helm, M. V. Kartsovnik, I. Sheikin, et al., Phys.Rev. Lett. **105**, 247002 (2010).
28. M. V. Kartsovnik, T. Helm, C. Putze, et al., New J. Phys. **13**, 015001 (2011).
29. J. Eun and Chakravarty, Phys. Rev. B **84**, 094506 (2011).
30. T. Helm, M. V. Kartsovnik, C. Proust, et al., Phys. Rev. B **92**, 094501 (2015).
31. A. A. Nikolaeva, L. A. Konopko, T. E. Huber, A. K. Kobylyanskaya, and G. I. Parai, Thermoelectricity, No. 4, 1607 (2015).
32. A. A. Nikolaeva, L. A. Konopko, A. V. Tsurkan, and E. F. Moloshnik, J. Surf. Eng. Appl. Electrochem. **52**, 2016 (2016).
33. R. Rousseau, M. L. Doulet, E. Canadell, R. P. Shibaeva, S. S. Khasanov, L. P. Rosenberg, N. D. Kusch, and E. B. Yagubskii, J. Phys. 1 **6**, 1527 (1996).
34. A. A. Slutskin, Sov. Phys. JETP **31**, 61 (1970).
35. A. A. Slutskin, Doctoral Dissertation (Phys. Tech. Inst. Low Temp., Acad. Sci. Ukr. SSR, Kharkov, 1980).

Translated by N. Wadhwa